EUROPEAN LABORATORY FOR PARTICLE PHYSICS

LHCb 2000–30
CALO
16 June 2000

MONTE-CARLO study of LHCb preshower

E. Guschin[a)], S. Laptev

Institute for Nuclear Research
Russian Academy of Sciences
60th October Anniversary Prospekt 7A
RU-117312 Moscow

LHCb Collaboration

Abstract

Results of LHCb preshower studies done with stand-alone Monte-Carlo programs are described. The main performances of PreShower detector, such as dynamic range, π/e rejection and energy corrections of ECAL response have been estimated for 1.5,2,2.5 and $3X0$ thicknesses of the PS absorber. Effect of light photo-statistics was also considered.

[a)] Corresponding author, E-mail: Evgueni.Gouchtchine@cern.ch

1 Introduction

SPD/Preshower detector is a part of calorimetry system in LHCb experiment. Main purpose of calorimetry system of LHCb is to provide $\gamma/e/\pi$ separation at the trigger level and off-line together with precise measurement of particles energy and position [1]. It consists of two layers of scintillator with Lead absorber plate in between. In order to optimise detector parameters, we study with stand-alone Geant3 based program the dependence of main performances on the lead absorber thickness and the photo-statistical fluctuations of the detector response. We will study further the following characteristics:

- π/e rejection.
- energy resolution with ECAL.
- MIP registration in SPD.

2 Geometry description and Geant cuts

The detector geometry simulated in the program is simplified version of the real design: two layers of scintillator of 15 mm thickness with the lead plate in between. In order to estimate the effect of lead thickness, it was changed from $1.5 - 3$ $X0$. The distance between last scintillator plate and ECAL body was 10 cm. ECAL was present mainly in part of simulations, concerning with the energy corrections study (sec. 3.4, 3.5). For the major part of the results in order to minimise CPU consumption ECAL was not simulated. It was also checked that the main results do not change by that. Geant cuts on electrons and photons were chosen at 10 KeV, in order to reproduce the very beginning of e-m shower process in considerable details. There were electrons and pions with $1, 2, 5, 10, 20, 50$ GeV energy simulated by 30 K events each.

3 Results

3.1 Energy deposited in absorber.

The main quantity playing role in the PS detector performance is the energy losses in the lead absorber. This is an invisible part of the parent particle energy, which can not be detected. Only some correlation of it's value with the signal in the PS scintillator layer provides a possibility for the ECAL response corrections. The precision obtained with such corrections is being described in sec.(3.4). The fig. 1 show the mean and r.m.s. of energy deposited in the lead absorber with various thickness. The effect on the ECAL energy resolution is shown on the bottom plot. It should be compared with the design value for ECAL alone without PS: $\sqrt{((10\%)^2/E + (1\%)^2)}$. The thickness

of 3 $X0$ of the lead will change the resolution to $\sim \sqrt{((12\%)^2/E)}$, if no correction is applied.

3.2 Energy deposited in PS and SPD scintillator.

The electron/pion separation is based on the fact that electrons produce shower starting in the absorber, and therefore a bulk of particles leaving the lead for scintillator gives signal values larger than the typical ones from hadron particles. From other hand, the PS signal is to be used for the energy corrections. Therefore the precision of the PS response measurement is an issue of detailed study. On the fig. 2 the mean and r.m.s. values of the energy deposit in PS scintillator versus electron energy are plotted. For less dependence on the statistical fluctuations everywhere in this note **r.m.s.** was calculated inside the window containing 99% of events with 0.5% of events left bellow and 0.5% above the window. On the plot one can see, that the response is increasing with the scintillator thickness, i.e. there is a factor of ~ 2 difference between 2 and 3 $X0$. On the bottom plot at the same figure the dynamic range, calculated as an upper boundary of spectrum containing 99% of events, is shown. The value of dynamic range is expressed in terms of MIP's response. Here and everywhere in this note the MIP's response is the most probable value of the minimum ionising particle signal in scintillator. The results on the dynamic range are in good agreement with experimental data obtained in [2], [3].

The SPD signals from electrons are not so different from the pions ones. As soon as SPD operates in registration mode, with threshold value about 0.5 MIP, there is no specific requirements on the photo-detector linearity and dynamic range defined by SPD. The most important is a requirement for the light yield, which is being discussed bellow.

3.3 π/e rejection

Evidently, the thicker is a lead absorber, the larger electron signal is in PS. While the signal from pions passing the absorber without interactions does not change. Therefore the π/e separation, potentially, can be improved with a larger lead thickness. On the fig. 3 one can see the accepted fraction of pions and rejected one of electrons plotted versus the PS threshold value for the various thicknesses of the lead at $1-50\ GeV$ beam energy. Provided the scale of the threshold axis is changed with energy, one can see relative changings of curves with energy and thickness. On the fig. 4 the π/e separation is shown for various values of PS threshold kept constant on the particle energy, that could be an option for the trigger application. There are 4 plots corresponding to 4 values of lead thickness: $1.5, 2, 2.5$ and 3 $X0$. It is clearly seen, that good pion rejection obtained for high energies is in contradiction with a high electron acceptance efficiency at low energies. One has to vary the threshold value by few times in order to gain in particle selection over all dynamic range. For off-line analysis one can tune the threshold with energy. The comparison of electron/pion

separation for various values of beam energy and the absorber thickness in case of adjustable PS threshold is shown on figure 5. One can see, that the pion rejection factor is better by $\sim 20-30\%$ with 3 $X0$ than with 2 $X0$ absorber thickness and is slightly increased with the energy.

3.4 Correction with PS signal the energy lost in absorber

As it was mentioned above, there is a correlation between an e-m shower energy lost in the absorber and the PS signal. The fig. 6 shows the scatter plot for 50 GeV electrons with the 2X0 thick lead. The energy lost in absorber in the first order approximation can be represented by PS signal linearly:

$$E_{corr} = E_{PS} * \kappa + E_0$$

It was found, see on fig. 7, that for given lead thickness the values of κ and E_0, in the first approximation, are constant on the beam energy (see table 1).

Table 1: The PS correction coefficients, taken as constants on the energy.

Lead thickness	κ	E_0,MeV
1.5 X0	1.5	20
2.0 X0	2.1	40
2.5 X0	2.7	70
3.0 X0	3.4	110

Due to the intrinsic fluctuations in an electromagnetic shower the energy lost in the absorber, in particular, at the low beam energies can be hardly corrected with PS signal (see fig. 8 and 9). To estimate the PS absorber effect with a realistic ECAL geometry, an other simulation was done with ECAL block of 20×20 cm^2 lateral dimension situated behind the PS at 10 cm. ECAL consists of 70 pairs of layers of 2 mm lead + 4 mm of scintillator. The PS absorber thickness was 2 $X0$. At that, to stress the effect of the presence of the PS absorber in front of the ECAL on the energy resolution of the later, the ECAL response was calculated as sum of energy deposit in the ECAL lead and scintillator components. After the PS correction of the energy absorbed in 2 $X0$ lead absorber the resolution of ideal ECAL was practically recovered at the energies above $5-10$ GeV. The overall effect from the 2 $X0$ absorber is not significant with respect to the ECAL design energy resolution of $10\%/\sqrt{(E)}$.

3.5 Correction with PS signal the energy lost in passive front material of ECAL

Becides the energy lost in the PS absorber, another significant part of shower energy is absorbed in the first passive layers of the ECAL mechanical structure. The case

of $3X0$ PS with Shashlik calorimeter starting with 2 mm inox plate was studied in [3]. Here we consider $2X0$ lead absorber in PS and, as an example, Shashlik ECAL with the front plate of 5 mm of iron plus an optional 2 mm of lead in front of first scintillator plate. General Monte-Carlo setup of PS and ECAL was the same as in 3.4. The ECAL response was computed as sum of signals from 70 scintillator layers. On the fig. 11 the mean and r.m.s. of e-m shower energy deposited in the PS absorber and front layers of ECAL is shown. One can see that energy lost in passive material is strongly dependent on the incident electron energy, and losses in each iron and lead plates in front of ECAL are almost equal to losses in PS $2X0$ absorber. This is a significant fraction of beam energy achieving 19% at 1 GeV (see left-hand plot on fig. 13) and it has to be reconstructed with PS. If no PS correction applied ECAL with all staff of passive material in front will has a strong nonlinearity of the response and energy resolution about 14% at 1 GeV. The energy lost in the passive material was linearly reconstructed with PS signal. The precision of the recontsruction of losses in the front plates of ECAL was found to be higher, then in the case of the same thickness of a passive material is added to PS absorber (see fig. 12). The effect of the PS corrections on the energy resolution of ECAL is shown on fig. 13. From these plots one can conclude the presence of even a minor passive material behind PS in front of ECAL affects significantly ECAL energy resolution and needs additional correction of ECAL response with PS signal. Of course, in the considered exercise the front 2 mm lead plate was taken for an additional exaggeration of the effect, and it is easy to start Shashlik sampling structure with scintillator layer. But nevertheless, it is an important to optimise the front mechanical structure of ECAL, especially in case of larger PS absorber thickness, when the effect grows up exponentially.

3.6 Effect of the light photo-statistics on the PS correction.

In the real world the PS signal is to be disturbed by photo-statistical fluctuations of the light collected from scintillator. Typical value of the light collected from MIP at the stage of photo-cathode is 20-30 ph.el [4]. This value is distributed by Poisson's law. In order to estimate of the effect of such fluctuations on the performance of the PS correction, we suppose, that corrected energy is disturbed in the first approximation around the value of an average PS response, neglecting the details of PS signal spectrum:

$$\delta E_{corr} = \delta < E_{PS} > *\kappa$$

This simply means that, in the case of average PS signal equals to 10 MIPs, we estimate the PS signal photo-statistical fluctuations as $\sqrt{(}10)$, and the corresponding fluctuations of the corrected energy to be equal $\sqrt{(}10) * \kappa$. The result of such estimation in case of 2 $X0$ lead thickness is shown on fig. 14. The black curve shows the intrinsic precision of the PS correction due to e-m shower nature. Due to the already big shower fluctuations, the PS correction itself is rather poor, and thus there is no noticeable contribution of the photo-statistical fluctuations.

3.7 Effect of the light photo-statistics on MIP registration in SPD.

As a performance most sensitive to the photo-statistical fluctuations, we study MIP registration efficiency in SPD. For this the energy deposit spectrum was convoluted with Poisson's distribution with respect to the light yield value. On the fig. 15 one can see the spectrum from MIPs in SPD obtained with $5, 10, 15, 20$ and 40 $ph.el./MIP$. The visible distortion of the low energy part of the spectrum causes the lower registration inefficiency for the given value of threshold applied. At the level of 0.5 MIP threshold the value of 15 $ph.el.$ for the light yield gives 1% of lost triggers.

4 Conclusions on SPD/PS performance requirements

From the results of simulations described above, we conclude that:

- The thickness of Lead absorber can be chosen about 2 $X0$, as a compromise between π/e rejection power and dynamic range of electronics. The later is being considered as a higher priority argument.
- The value of the light yield per MIP is to be larger then 15 $ph.el.$ for the reliable MIP registration in SPD. The precision of the correction the energy lost in lead absorber by the use of the PS signal is not affected by the photo-statistical fluctuations in case of realistic light collection.
- The presence of 2 $X0$ lead absorber in front of ECAL spoils the ECAL energy resolution as $\sim 4\%/\sqrt{(E)}$ to be added quadratically to the ECAL design value of $\sim 10\%/\sqrt{(E)}$. This effect can be corrected significantly by the PS signal over $5 - 10$ GeV energy.
- Even small amount of passive material behind PS in front of ECAL, like few millimeters of iron, absorbes significant fraction of e-m shower energy. The effect is strongly dependent on a shower energy and rises up exponentially with PS absorber thickness. It has to be also reconstructed with PS signal.

References

[1] LHCb Collaboration, "LHCb Technical Proposal", CERN/LHCC 98-4 (1998).

[2] P.Perret et al., "LHCb PS signal characteristics", LHCb 2000-026, CALO

[3] RD36 Collaboration, "Energy and spatial resolution of a Shashlik Calorimeter and a Silicon Preshower Detector", CERN-PPE/95-151.

[4] Yu.Gavrilov *et al*, "Experimental performance of SPD/PS prototypes", LHCb 2000-031, CALO.

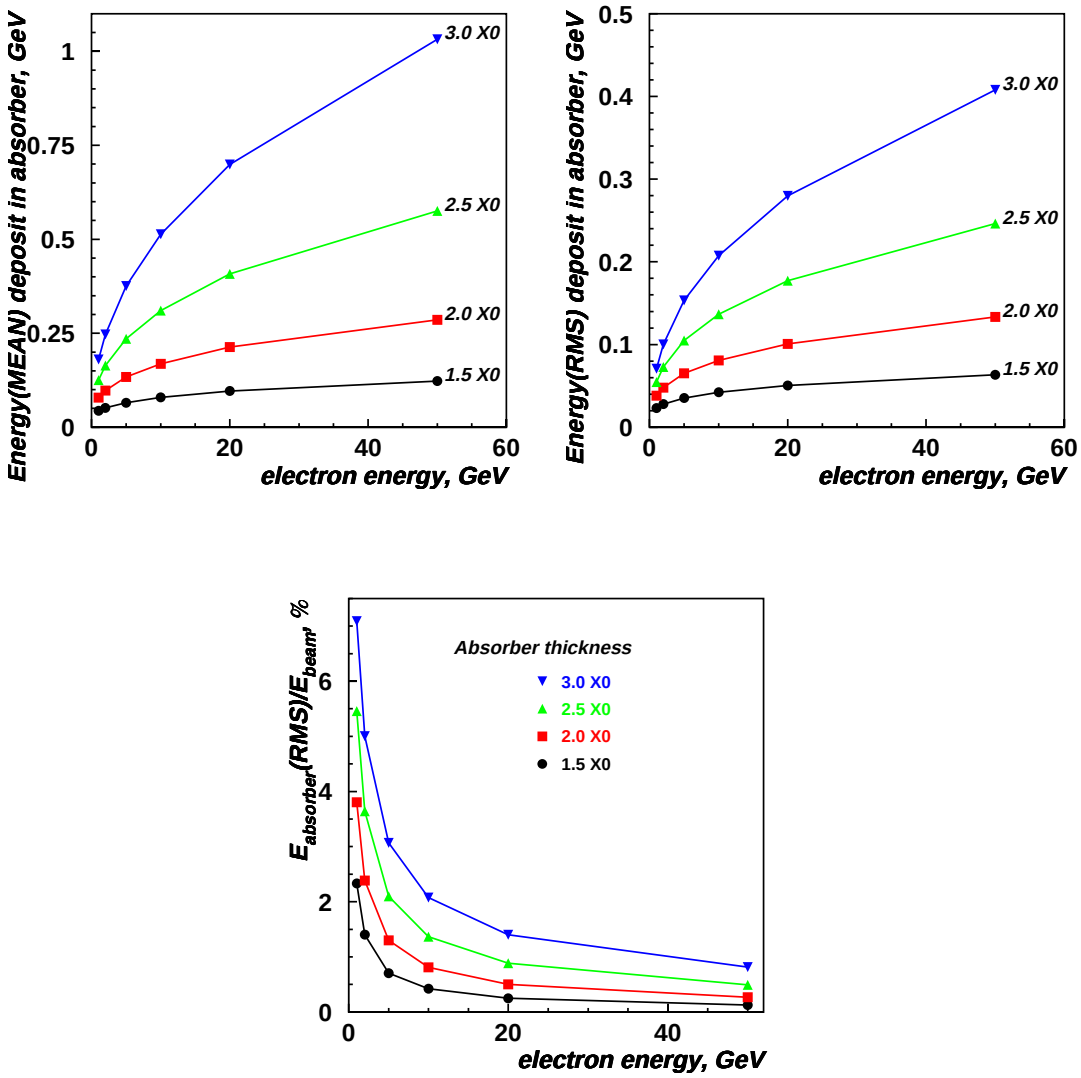

Figure 1: Energy lost in Lead by electrons of $1-50\ GeV$. Upper left-hand plot shows the mean values vs electron energy. On the right plot the standard deviation is represented. The thickness of lead was changed to $1.5, 2, 2.5$ and $3\ X0$. On the lower plot the relative error on the energy measurement is shown. This should be compared with design ECAL resolution of $10/\sqrt{(E)} \oplus 1, \%$. For the larger thickness values of $2.5-3\ X0$ the effect becomes not negligible.

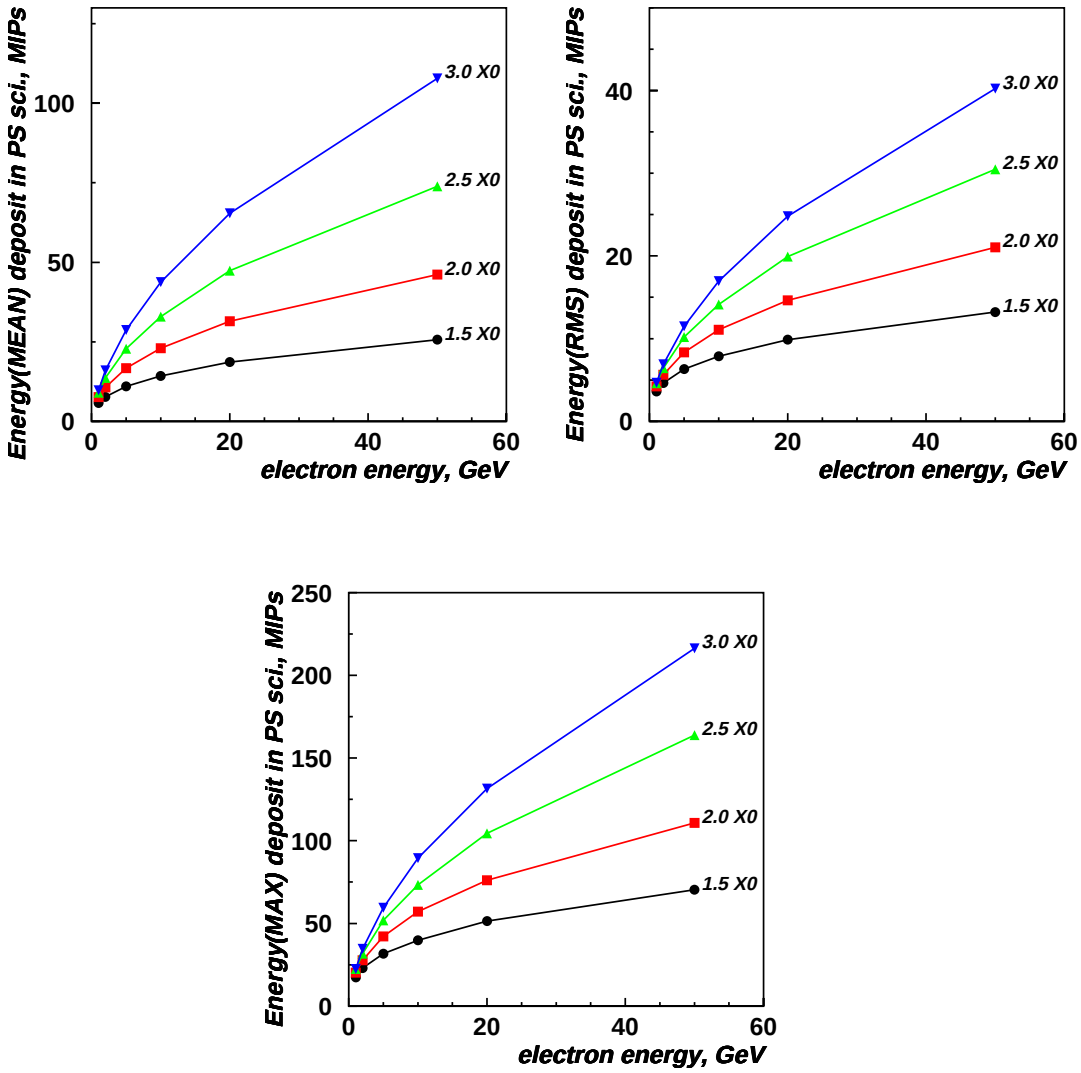

Figure 2: Energy deposited in PS scintillator by electrons of 1-50 GeV is shown. Upper left plot shows the mean values vs electron energy, and the standard deviation is represented on the right plot. The thickness of the lead was varied between $1.5, 2, 2.5$ and 3 $X0$. On the lower plot the dynamic range is shown, defined as a range containing 99% of PS signal. The factor of 2 difference is calculated between 2 and 3 $X0$ lead thickness values.

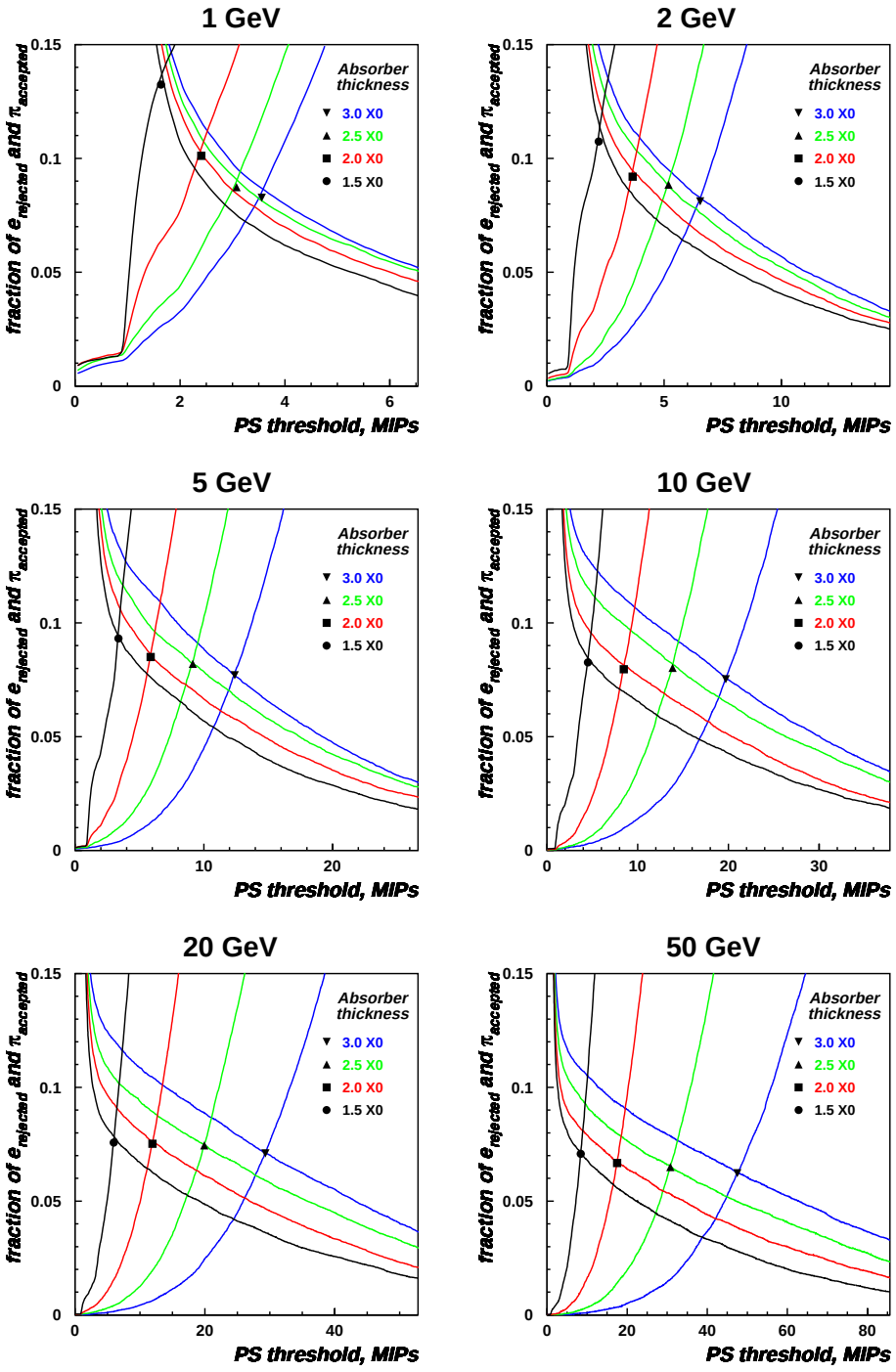

Figure 3: π/e rejection in PS. Each plot shows two curves per one value of the absorber thickness for given energy of the beam particles: a fraction of pions accepted is dropping with PS threshold increase, and a fraction of electrons bellow the threshold is correspondingly growing up. One can see insignificant improvement in the pion rejection power with a thicker absorber at large energies.

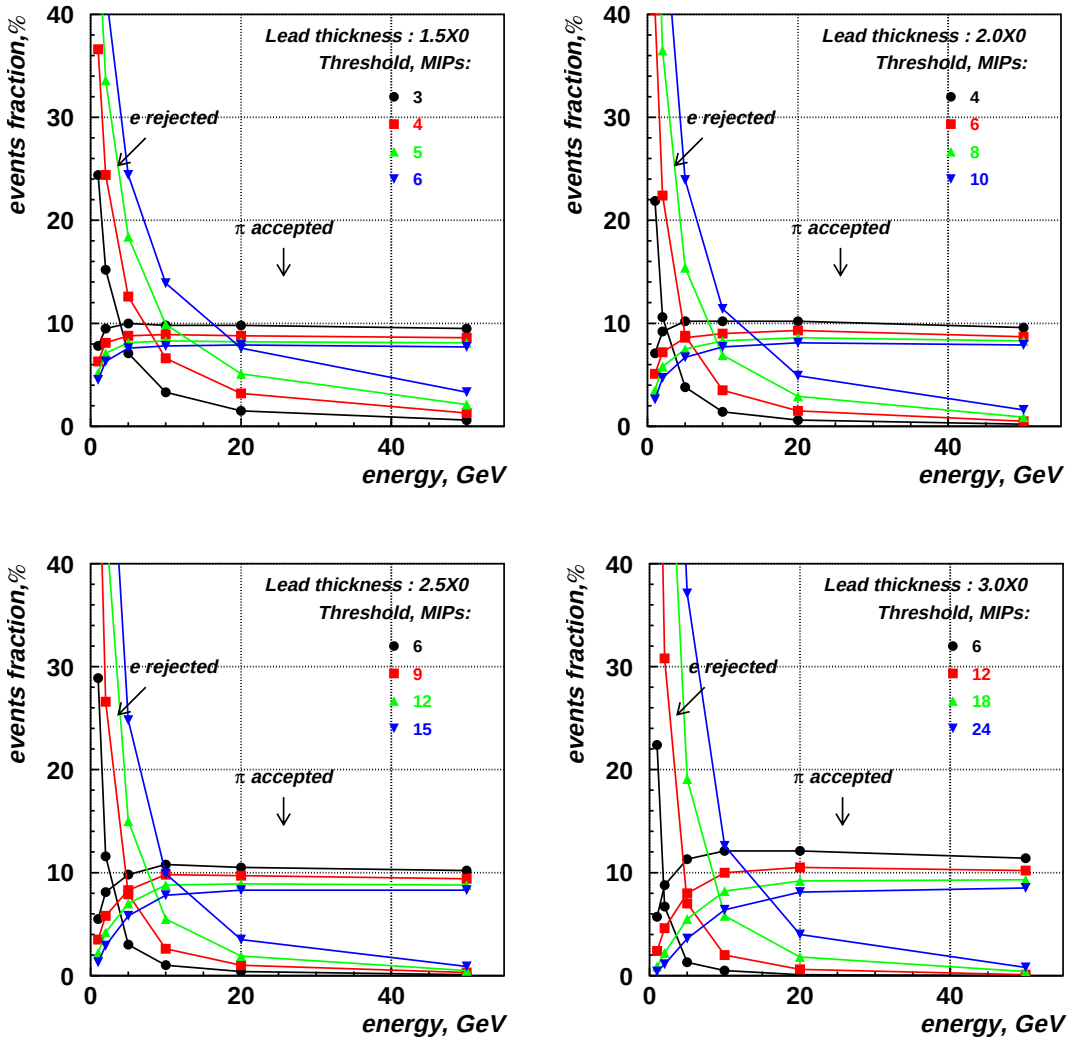

Figure 4: π/e rejection in PS for constant value of the threshold. To obtain both good pion rejection and high electron acceptance over all energy scale, one has to vary the threshold value with the beam energy.

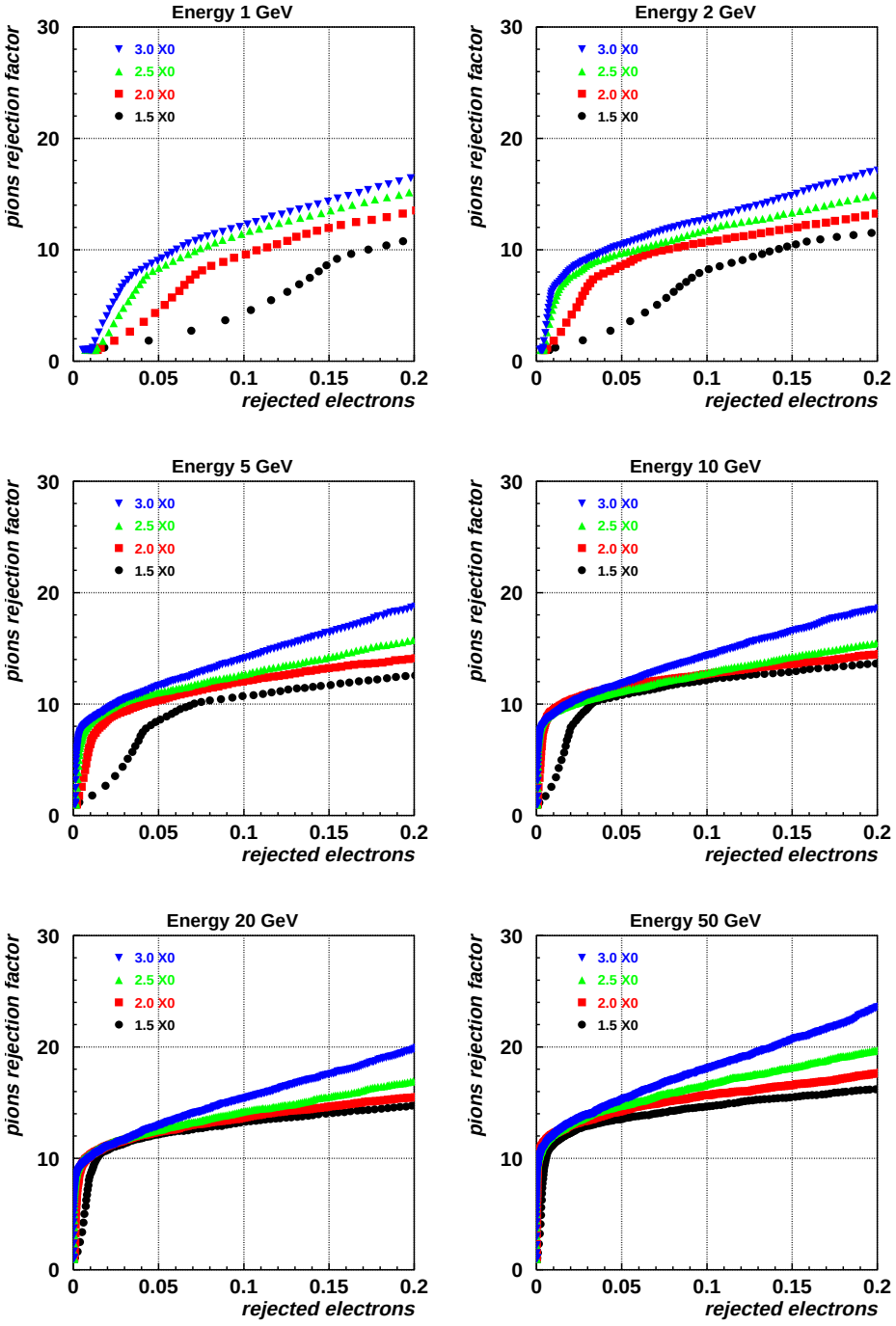

Figure 5: π/e rejection in PS with the threshold tuned with energy. The electrons and pions energy was changed from 1 to 50 GeV. If 10% of electrons is rejected, the pion rejection factor is larger by $20-30\%$ for 3 $X0$ lead thickness than for 2 $X0$. It also can be seen, that the pion rejection is larger for high energies.

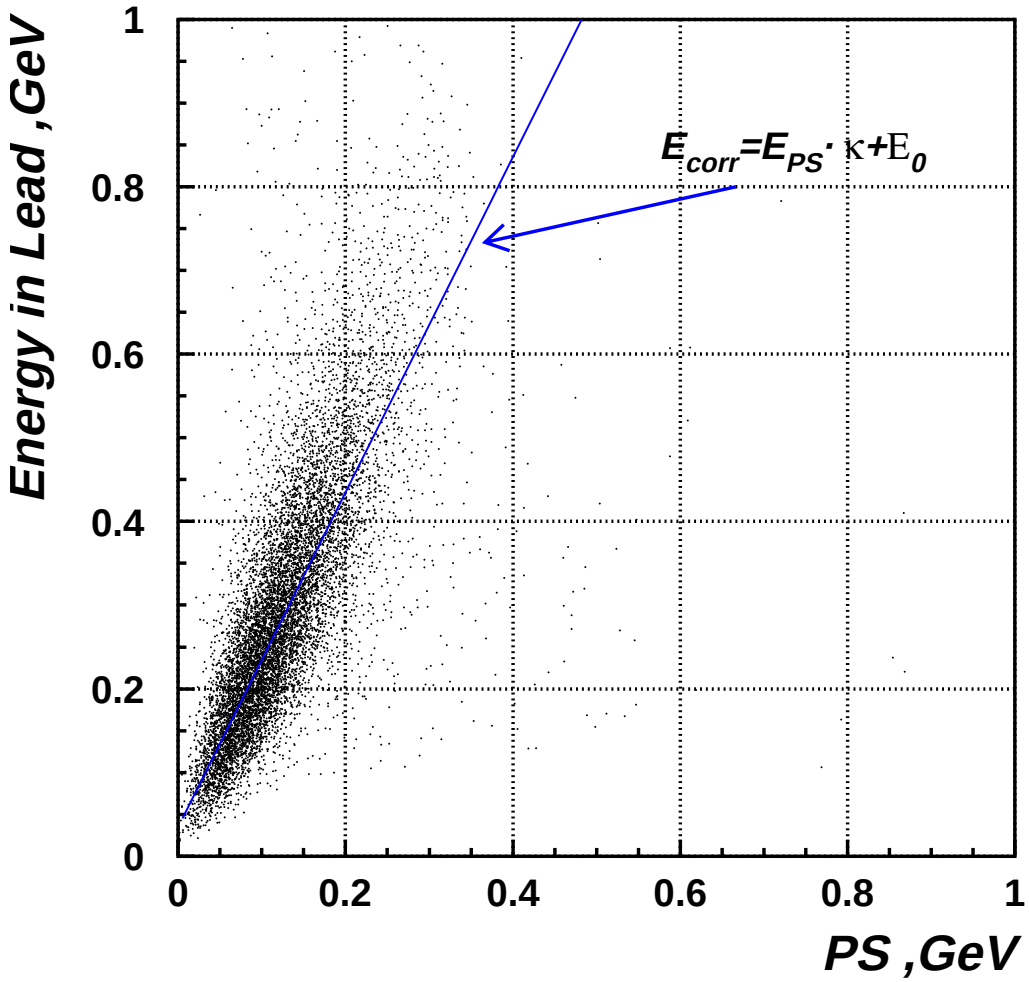

Figure 6: Energy of the electro-magnetic shower lost in the lead absorber is plotted versus PS signal. The shown correlation is to be used for correction of energy losses. Linear correction is being a good approximation.

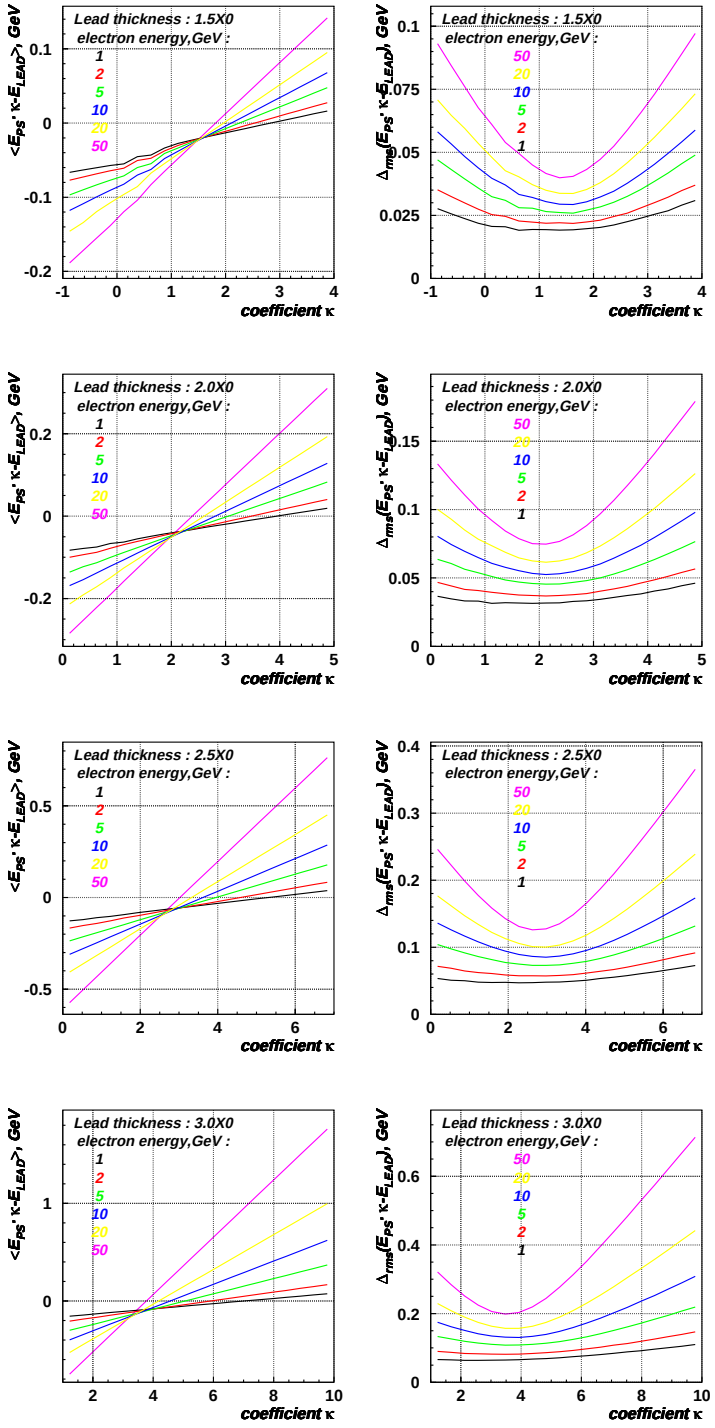

Figure 7: Linear correction is being a good approximation for all considered values of lead thickness and beam energy. At the left-hand column each diagram shows the mean value of $E_{lead} - E_{PS} * \kappa$ plotted vs value of κ coefficient. For all beam energies the corresponding lines cross about at the same point (E_0, κ) at the value of κ, resulting to the minimal variance $\delta(E_{PS} * \kappa - E_{lead})$ (right column). Thus the coefficients E_0, κ of linear correction for given value of absorber thickness in the first approximation are not dependent on the energy.

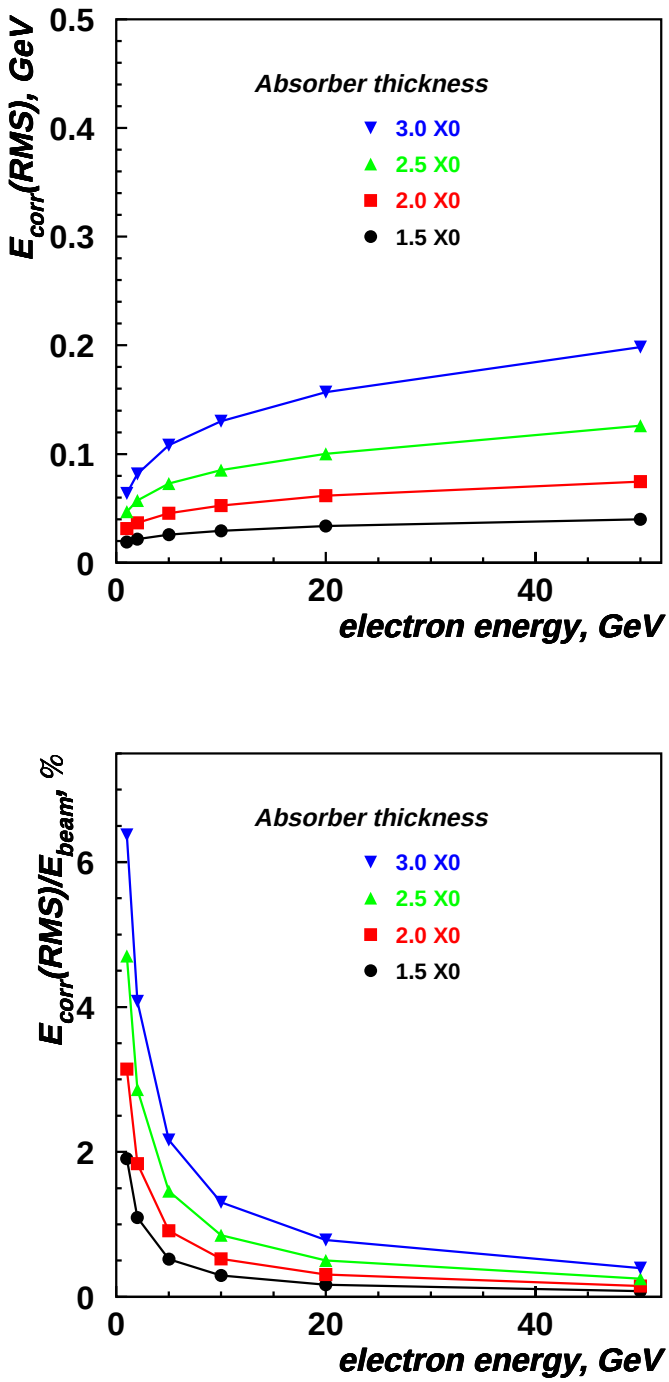

Figure 8: Error of the correction of energy losses in absorber with PS signal $\delta(E_{corr} - E_{lead}), r.m.s.$, where $E_{corr} = E_{PS} * \kappa - E_0$, is shown on the upper plot. The lower plot shows resulting error to the ECAL energy resolution.

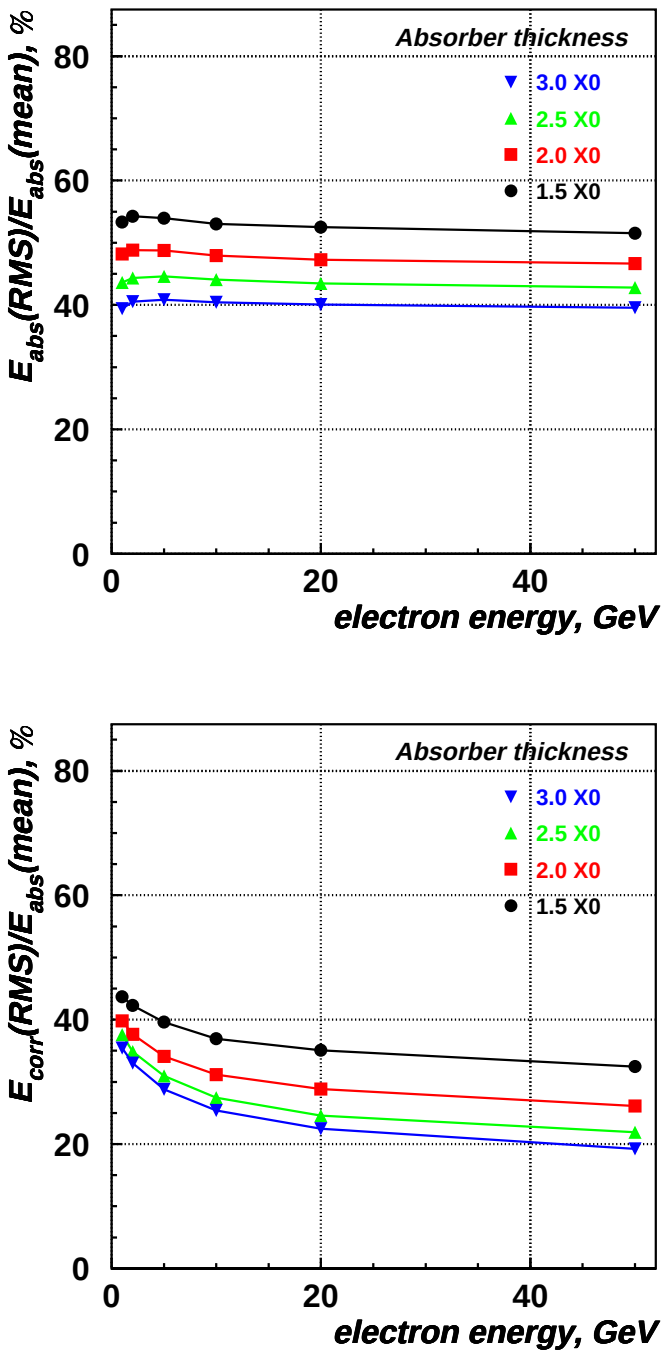

Figure 9: Ratio of the fluctuations (r.m.s.) of the energy lost in the lead absorber to its mean value is plotted vs beam energy on the top figure. On the bottom one can see the same data after the correction with PS signal. From comparison it can be concluded, that the PS correction works more efficiently at higher energies.

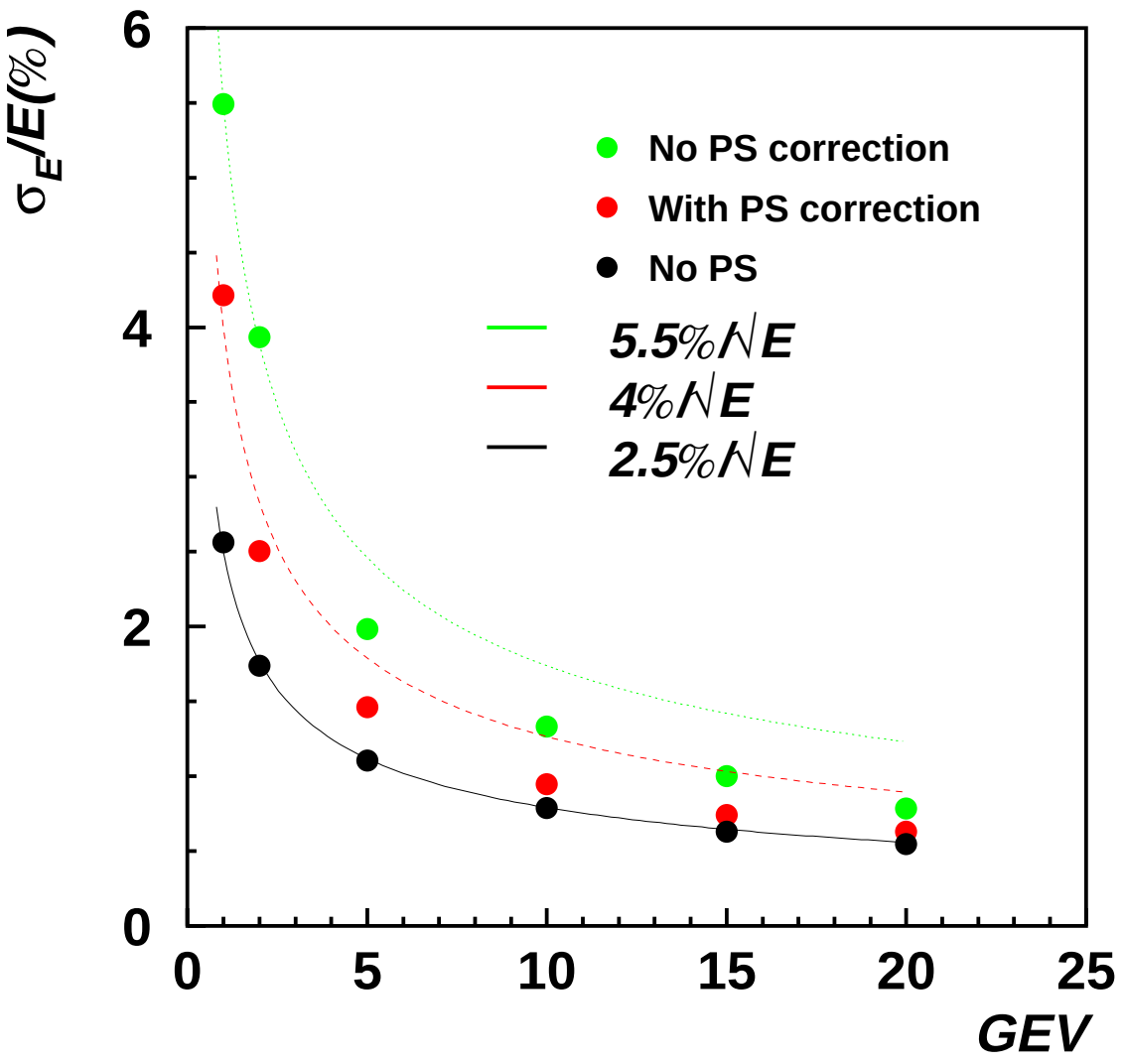

Figure 10: The same as previous fig. 8, but simulation was done with an ideal ECAL at 10 cm behind the PS. Lead thickness was 2 $X0$. The ECAL response was taken as a sum of energy deposit in both lead and scintillator components of ECAL in a lateral dimension of 20×20 cm^2, as some realistic approach. Therefore the lateral leakage of an e-m shower contributes to the energy resolution at the level of $2.5\%/\sqrt{(E)}$ (bottom curve). Without PS correction the resolution curve (green dots) is between 5.5 and $4\%/\sqrt{(E)}$. Corrected by PS signal, it is in between 4 and 2.5%. At the energies above 10 GeV, the PS correction is very efficient.

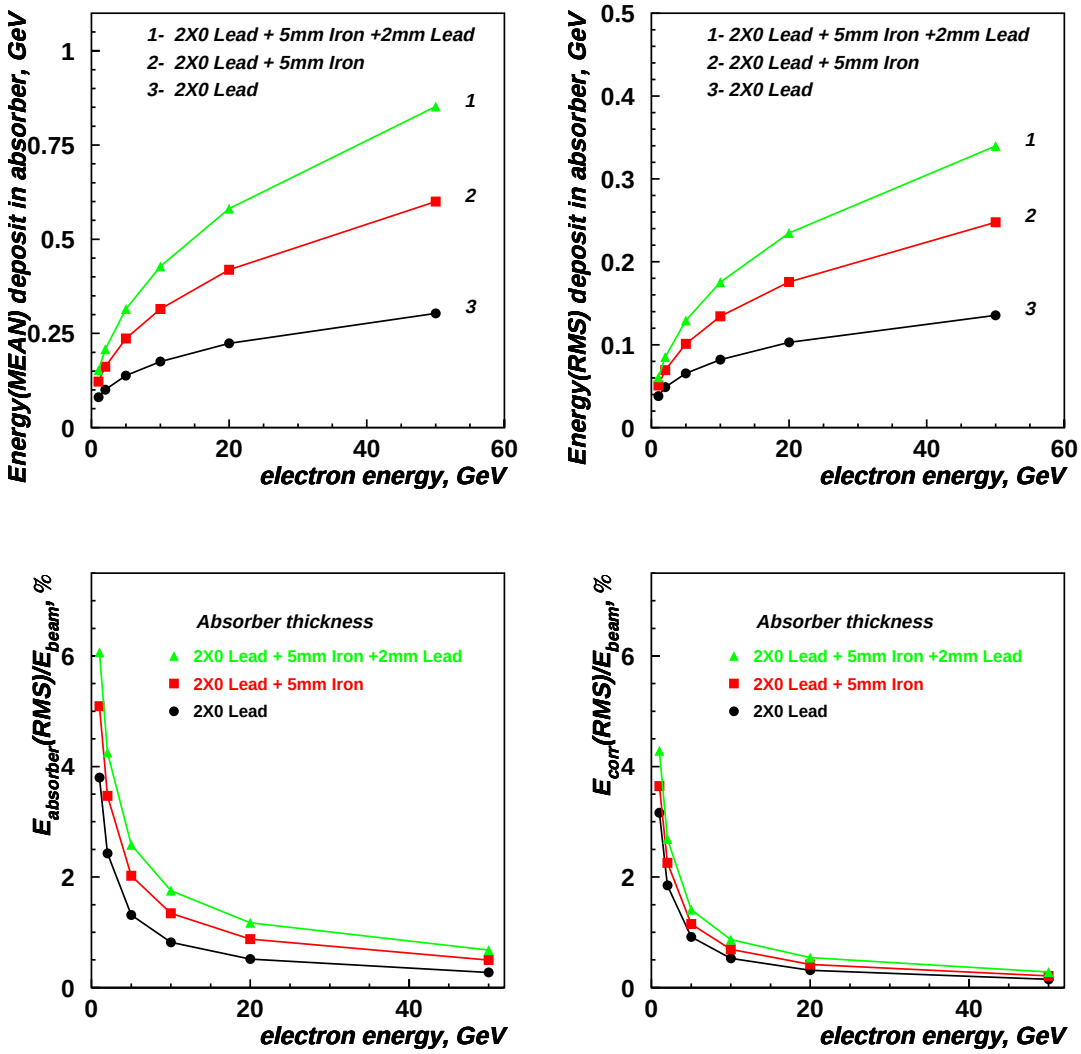

Figure 11: The energy absorbed in the passive material in front of ECAL is shown. As an example of ECAL front plates design, a 5 mm steel was taken as an element of mechanical construction and a 2 mm lead plate is the first plate of Shashlik sampling structure. The e-m shower energy lost in each of these two plates is almost equal to losses in PS converter of $2X0$ lead. Ratio of lost energy fluctuations to the beam energy before and after PS corrections is shown at the bottom plots.

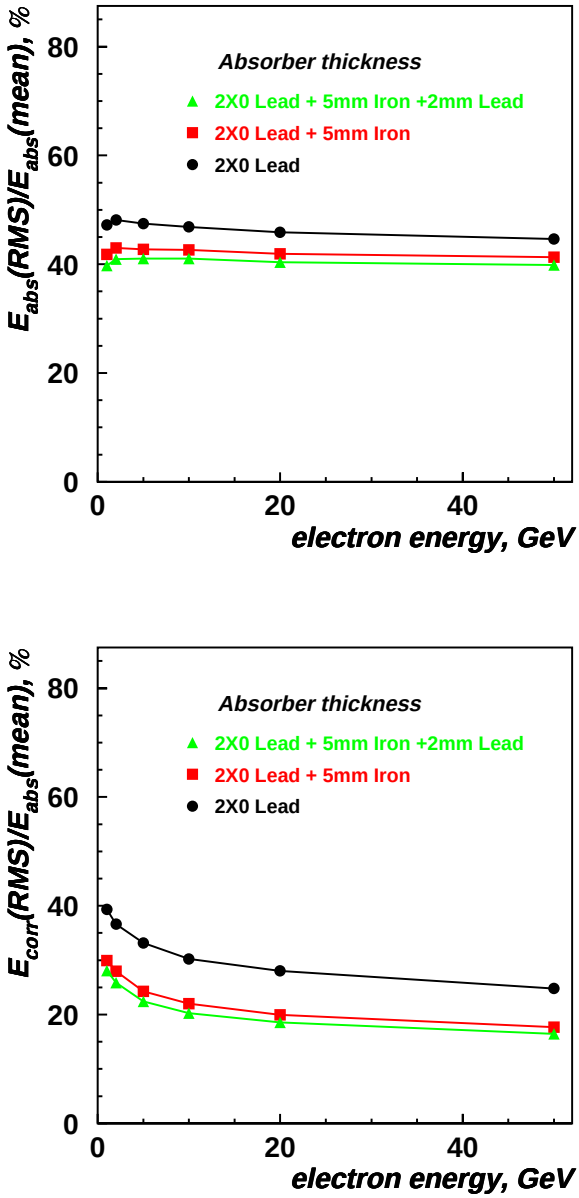

Figure 12: Ratio of the fluctuations (r.m.s.) of the energy lost in the lead absorber and in the passive material of ECAL to its mean value is plotted vs beam energy on the top figure. The same data after the correction with PS signal are shown on the bottom plot. From comparison with fig. 9 one can see that the correction works better for the front material of ECAL then for an additional absorber of PS.

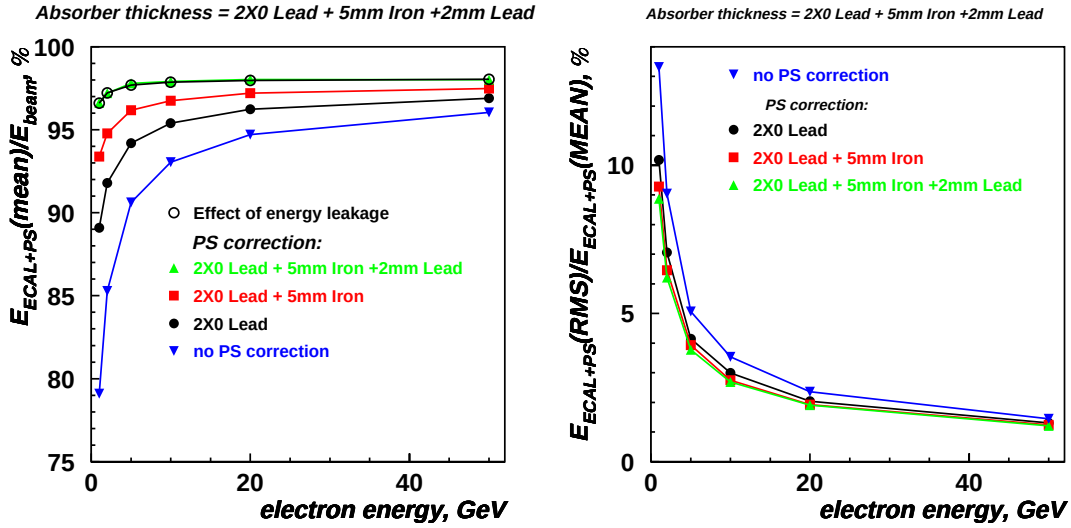

Figure 13: To account all the effects of PS together with the passive material (5 mm steel + 2 mm the first lead layer) in front of the first scintillator layer of ECAL, detailed simulation of ECAL sampling structure with 4 mm scintillator and 2 mm lead (70 layers of each) was done. Lateral dimensions of ECAL block were 20 cm cm. One can see on the left-hand plot the ratio of the reconstructed ECAL energy to the beam energy in cases, when PS correction was applied for energy lost in $2X0$ lead absorber, absorber + 5 mm steel and absorber + 5 mm steel + first lead layer of ECAL. The significant fraction of shower energy lost in passive material before the first scintillator layer in ECAL is strongly dependent on the beam energy and can be sufficiently corrected with PS signal. After the PS correction applied to energy lost in PS abosrber + passive front layers the ECAL energy is reconstructed completely and coincides with the shower leakage curve, shown as upper one. On the right plot the energy resolution obtained with ECAL with and without PS corrections is shown. The correction of energy lost in front passive layers of ECAL improves the overall energy resolution.

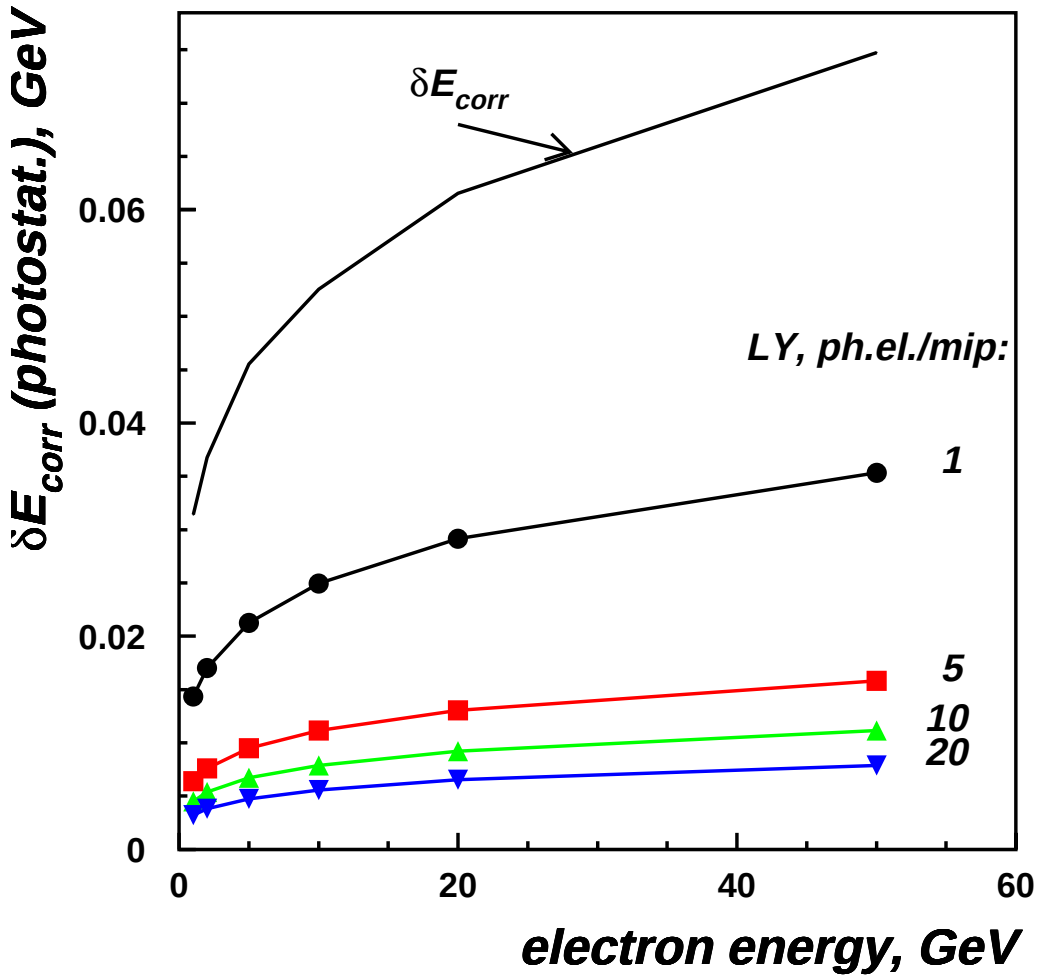

Figure 14: The contribution of light photo-statistics to the PS correction precision was found to be small even if light collection is extremely small, as 1 $ph.el./MIP$. The light photo-statistics contribution is plotted vs the beam energy in the case of 2 $X0$ lead thickness. By the upper black curve an intrinsic precision of the PS correction, defined by the e-m shower fluctuations, is shown for comparison.

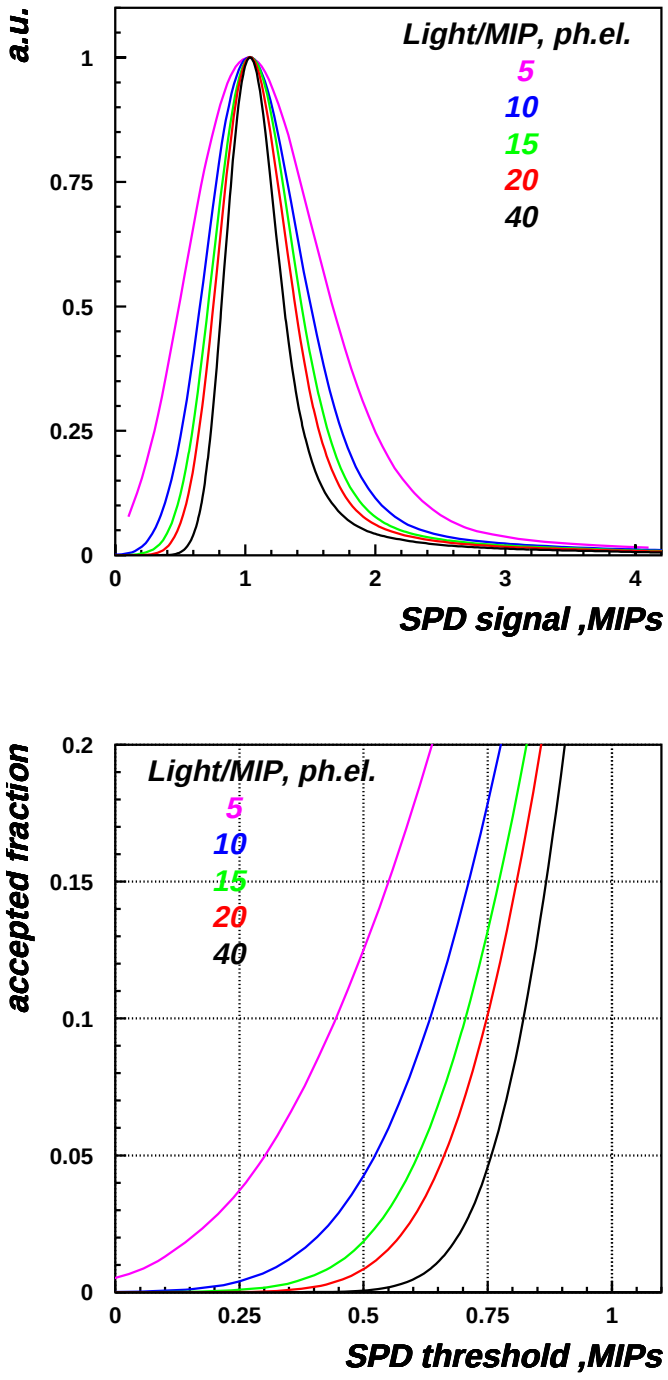

Figure 15: The effect of light photo-statistical fluctuations on the MIP registration in SPD is shown. On the upper plot one can see the distortion of SPD spectrum in case of $5, 10, 15, 20$ and 40 *ph.el.* collected per MIP. The MIP registration inefficiency as function of applied threshold is demonstrated on the bottom plot.